

# NUMERICAL SIMULATION OF BLOOD FLOW AND CHOLESTEROL DISTRIBUTION FOR MIDDLE CEREBRAL ARTERY WITH COARCTATION

Masashi Naito, Kensaku Mizoguchi, Youhei Takagi, Yasunori Okano

## Abstract:

In order to understand of coarctation growth mechanism in a blood tube, numerical analysis for blood flow and cholesterol distribution in a blood tube was carried out. Numerical results showed that back flow existed behind the coarctation, and it was found that high blood pressure (HBP), and nonelastic conditions increased the cholesterol concentration behind the coarctation.

**Keywords:** numerical simulation, blood flow, coarctation, cholesterol distribution.

## 1. Introduction

Because of the recent development of medical equipments, early detection of vessel disease in a brain and cure can be realized. However, judgment of disease condition strongly depends on doctor's skill and experience, and an objective criterion for treatment is strongly demanded. Therefore, it is required to investigate causes and prevention of the disease from engineering view points such as fluid dynamics and mass transfer. However, it is difficult to model the property of vessel experimentally. Therefore, numerical simulation by using high performance computers must be a useful tool for it.

A coarctation, which is inflamed vessel wall, is a vessel disease. This phenomenon blocks the blood flow, and the growth of coarctation causes other diseases. In general, it is well known that cholesterol distribution plays an important role in the growth of coarctation.

Torii *et al.* [1] have reported the effect of blood pressure on aneurysm. Their model included the effect of vessel wall movement on normal blood pressure (NBP) and HBP. Kim and Ley [2] considered the cooling effect of blood over inflamed atherosclerotic plaque. However, the blood pressure effect and cholesterol distribution were not considered in their analysis. Sugawara *et al.* [3] investigated the relation between the intravascular pressure and the diameter of the carotid artery in six patients. These results showed the relationship between pressure and diameter was relatively linear throughout the cardiac cycle. Therefore, it was found that movement of vessel wall was expressed by a mathematical equation.

The final goal of this study is the development of simulation code for understanding of coarctation growth, which can be used for protection of blood tube disease. As the first step, the two-dimensional simulation code that can analyze the effect of blood flow and cholesterol distribution on a coarctation has been developed.

## 2. Model description and numerical procedure

### 2.1. Model description

Figures 1 and 2 show an analysis area and schematic model, respectively. In this study, the middle cerebral artery (MCA) that had a coarctation with ratio of 30 % was simulated under different vessel conditions; (a) is NBP and elastic, (b) is NBP and nonelastic and (c) is HBP and elastic.

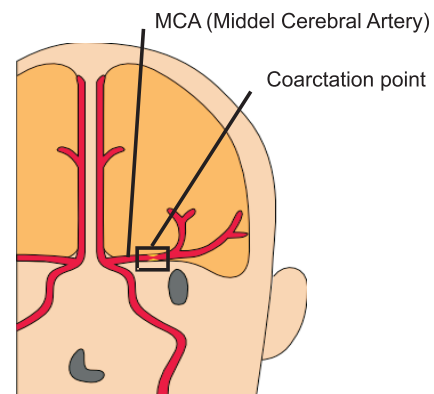


Fig. 1. Analysis area and coarctation point.

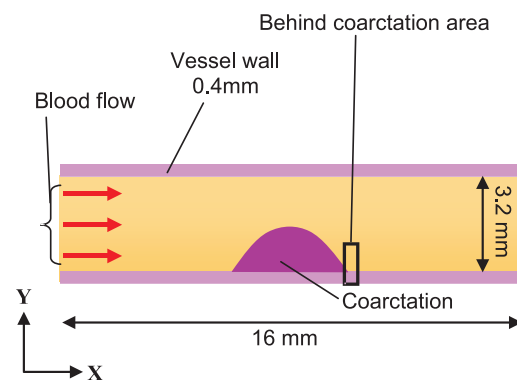


Fig. 2. Schematic model of MCA with coarctation.

### 2.2. Governing equations

The governing equations for the flow in the blood tube are the following continuity (1), Navier-Stokes (2), (3) and diffusion (4) equations;

$$\frac{\partial \mathbf{u}}{\partial x} + \frac{\partial \mathbf{v}}{\partial y} = 0, \quad (1)$$

$$\frac{\partial \mathbf{u}}{\partial t} + \mathbf{u} \frac{\partial \mathbf{u}}{\partial x} + \mathbf{v} \frac{\partial \mathbf{u}}{\partial y} = -\frac{1}{\rho} \frac{\partial p}{\partial x} + \nu \left( \frac{\partial^2 \mathbf{u}}{\partial x^2} + \frac{\partial^2 \mathbf{u}}{\partial y^2} \right), \quad (2)$$

$$\frac{\partial \mathbf{v}}{\partial t} + \mathbf{u} \frac{\partial \mathbf{v}}{\partial x} + \mathbf{v} \frac{\partial \mathbf{v}}{\partial y} = -\frac{1}{\rho} \frac{\partial p}{\partial y} + \nu \left( \frac{\partial^2 \mathbf{v}}{\partial x^2} + \frac{\partial^2 \mathbf{v}}{\partial y^2} \right), \quad (3)$$

$$\frac{\partial c}{\partial t} + u \frac{\partial c}{\partial x} + v \frac{\partial c}{\partial y} = D \left( \frac{\partial^2 c}{\partial x^2} + \frac{\partial^2 c}{\partial y^2} \right). \quad (4)$$

These equations were transformed into a dimensionless form as follows:

$$\frac{\partial U}{\partial X} + \frac{\partial V}{\partial Y} = 0, \quad (5)$$

$$\frac{\partial U}{\partial \tau} + U \frac{\partial U}{\partial X} + V \frac{\partial U}{\partial Y} = -\frac{\partial P}{\partial X} + \left( \frac{\partial^2 U}{\partial X^2} + \frac{\partial^2 U}{\partial Y^2} \right), \quad (6)$$

$$\frac{\partial V}{\partial \tau} + U \frac{\partial V}{\partial X} + V \frac{\partial V}{\partial Y} = -\frac{\partial P}{\partial Y} + \left( \frac{\partial^2 V}{\partial X^2} + \frac{\partial^2 V}{\partial Y^2} \right), \quad (7)$$

$$\frac{\partial C}{\partial \tau} + U \frac{\partial C}{\partial X} + V \frac{\partial C}{\partial Y} = \frac{1}{Sc} \left( \frac{\partial^2 C}{\partial X^2} + \frac{\partial^2 C}{\partial Y^2} \right). \quad (8)$$

Dimensionless number are as follows:

$$U = u \frac{v}{L}, \quad V = v \frac{v}{L}, \quad X = \frac{x}{L}, \quad Y = \frac{y}{L},$$

$$\tau = t \frac{L^2}{\nu}, \quad P = p \frac{\rho \nu^2}{L^2}, \quad C = \frac{c}{c_0}, \quad Sc = \frac{\nu}{D}. \quad (9)$$

They were discretized by the finite difference method, and solved by HSMAC method. Physical properties of blood were used for the calculation and Schmidt number was assumed to be 1000. Because vessel diameter was relatively large and flow rate was high, blood was assumed to be Newtonian fluid [1]. Mesh number and time step were set to be  $(x,y) = (200,50)$  and  $1.0 \times 10^{-6}$  second, respectively.

### 2.3. Boundary condition

Velocity in the inflow boundary was given by Fourier series expansion by using the flow rate obtained by ultrasound Doppler [4]. Fourier series expansion of inflow boundary can be written as follows:

$$u_i(t) = \frac{a_0}{2} + \sum_{n=1}^N (a_n \cos nt + b_n \sin nt) \quad (10)$$

where  $a_0$  is the modification coefficient;  $a_n$  and  $b_n$  are the Fourier cosine coefficient and Fourier sine coefficient of the  $n$ -th term;  $t$  is the time.  $a_0$ ,  $a_n$  and  $b_n$  are expressed as

$$a_0 = 0.257, \quad (11)$$

$$a_n = [-0.27 \sin(0.1n\pi) + 0.17 \sin(0.3n\pi) + 0.15 \sin(0.5n\pi) - 0.1 \sin(0.7n\pi) + 0.08 \sin(1.1n\pi) + 0.07 \sin(2n\pi)]/n\pi, \quad (12)$$

$$b_n = [0.1 + 0.27 \cos(0.1n\pi) - 0.17 \cos(0.3n\pi) - 0.15 \cos(0.5n\pi) + 0.1 \cos(0.7n\pi) - 0.08 \cos(1.1n\pi) - 0.07 \cos(2n\pi)]/n\pi. \quad (13)$$

Figure 3(a) shows inlet time-dependent blood flow. In this case Reynolds number changes between 80 and 380.

### 2.4. Movement of vessel wall

For the movement of vessel wall, the following three steps were considered. Firstly, stress at the vessel wall was calculated by using the following equation:

$$\sigma = \frac{r \cdot \Delta P}{h} \quad (14)$$

where  $\Delta P$  is expressed as  $\Delta P = P_{blood} - P_{base}$ .  $P_{blood}$  is time dependent blood pressure value, which was determined by the inlet flow. Therefore, the blood pressure is expressed by using Fourier series equation (Eq. (10)).  $a_0$ ,  $a_n$  and  $b_n$  are expressed as follows:

*NBP (Normal blood pressure)*

$$a_0 = 174.5, \quad (15)$$

$$a_n = [-35 \sin(0.1n\pi) + 20 \sin(0.3n\pi) + 30 \sin(0.5n\pi) - 20 \sin(0.7n\pi) + 10 \sin(1.1n\pi) + 80 \sin(2n\pi)]/n\pi, \quad (16)$$

$$b_n = [85 + 35 \cos(0.1n\pi) - 20 \cos(0.3n\pi) - 30 \cos(0.5n\pi) + 20 \cos(0.7n\pi) - 10 \cos(1.1n\pi) - 80 \cos(2n\pi)]/n\pi. \quad (17)$$

*HBP (High blood pressure)*

$$a_0 = 233.3, \quad (18)$$

$$a_n = [-62 \sin(0.1n\pi) + 35 \sin(0.3n\pi) + 40 \sin(0.5n\pi) - 25 \sin(0.7n\pi) + 15 \sin(1.1n\pi) + 105 \sin(2n\pi)]/n\pi, \quad (19)$$

$$b_n = [85 + 35 \cos(0.1n\pi) - 20 \cos(0.3n\pi) - 30 \cos(0.5n\pi) + 20 \cos(0.7n\pi) - 10 \cos(1.1n\pi) - 80 \cos(2n\pi)]/n\pi. \quad (20)$$

In this study, the physiological ranges for NBP and HBP are assumed to be 70-120 mmHg and 100-180 mmHg, respectively.  $P_{base}$  was set to be 100 mmHg. This value shows radius of standard vessel. Figure 3 (b) shows the pressure waveforms for the HBP and NBP conditions. Secondary, strain can be obtained as follows:

$$\varepsilon = \frac{\sigma}{E} \quad (21)$$

$E$  denotes a Young's modulus which was assumed to be  $10^5$ . Thirdly, deformation value of vessel wall is calculated by using radius of vessel and strain as follows:

$$L_{\text{movement}} = r\varepsilon \quad (22)$$

Figure 4 shows time dependent deformation value of vessel. The Maximum deformation value of vessel is 0.424 mm (HBP) and 0.228 mm (NBP).

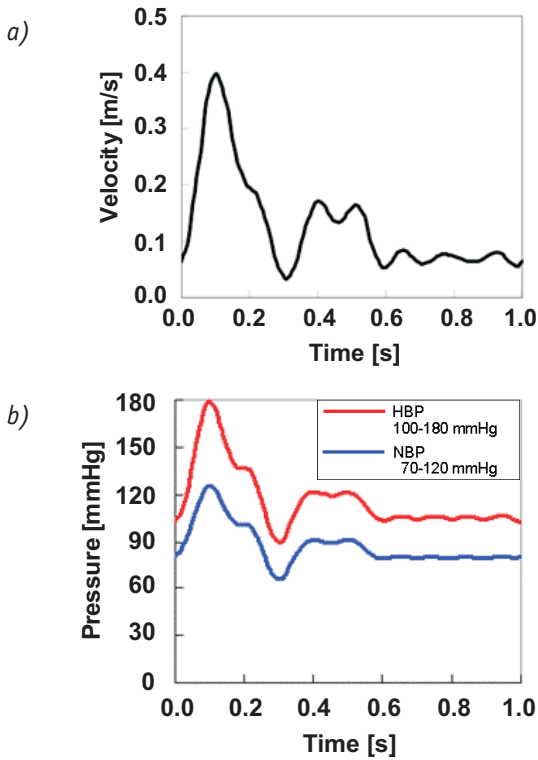


Fig. 3. Inlet timedependent blood flow (a) and blood pressure wave form (b).

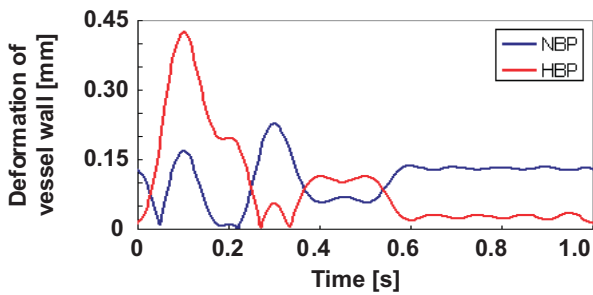


Fig. 4. Time dependent deformation value of vessel wall HBP and NBP

### 3. Results and discussion

Figure 5 shows the effect of vessel condition on velocity distribution at peak systole.

The inlet maximum velocity is called as “peak systole” ( $t = 0.1$  s). The results show fast velocity area appears on the top of the coarctation and reverse flow appears behind the coarctation. When the vessel diameter expands at peak systole, distance between the coarctation and vessel wall becomes wider. However, the vessel diameter in the case (b) keeps constant value. In (b), distance between the coarctation and vessel wall becomes narrow and the fastest velocity appears above the coarctation.

Figure 6 illustrates the effect of vessel condition on cholesterol distribution at peak systole.

Mostly cholesterol is transported by blood flow because of high Schmidt number system. Figure 5 shows that reverse flow appears behind coarctation area. Therefore, cholesterol is transported by the reverse flow and cholesterol accumulated these area. Also, (c) has the highest cholesterol concentration.

Figure 7 shows the effect of vessel condition on velocity distribution at peak diastole.

The inlet minimum velocity is called as “peak diastole”. When the vessel diameter decreases at peak diastole, distance between the coarctation and vessel wall becomes narrow. Fast velocity area appears on the top of the coarctation and the reverse flow appears behind the coarctation, same as the case of peak systole as shown in Figure 5.

Figure 8 indicates the effect of vessel condition on cholesterol distribution at the peak diastole.

Cholesterol is transported by the reverse flow similar to the case of peak systole, and this phenomenon enhances growth of coarctation. Also, cholesterol concentration was increased under HBP and nonelastic conditions.

Effect of vessel condition on cholesterol distribution in one cycle is shown in Figure 9.

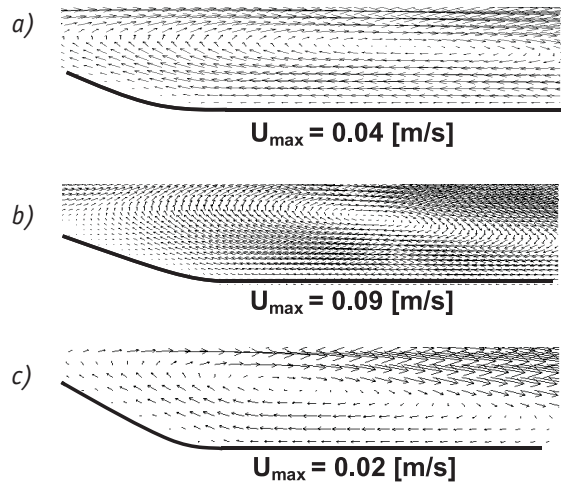
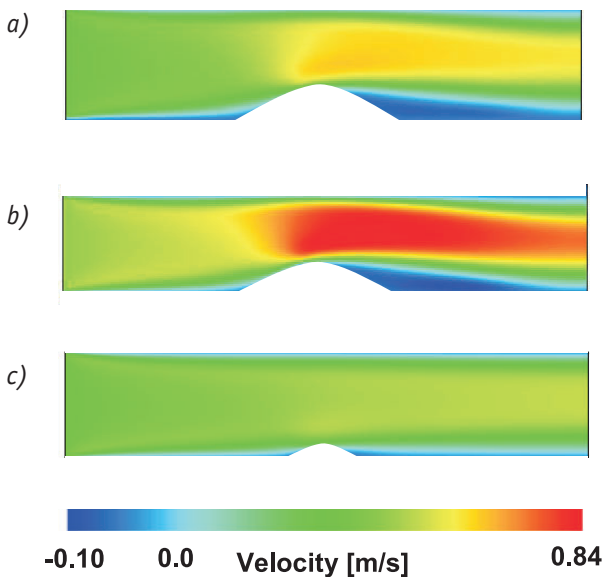


Fig. 5. Effect of vessel condition on velocity distribution (left) and its enlarged view in “behind coarctation area” shown in Fig. 2 at peak systole (right). (a) NBP and elastic vessel, (b) NBP and nonelastic vessel and (c) HBP and elastic vessel.

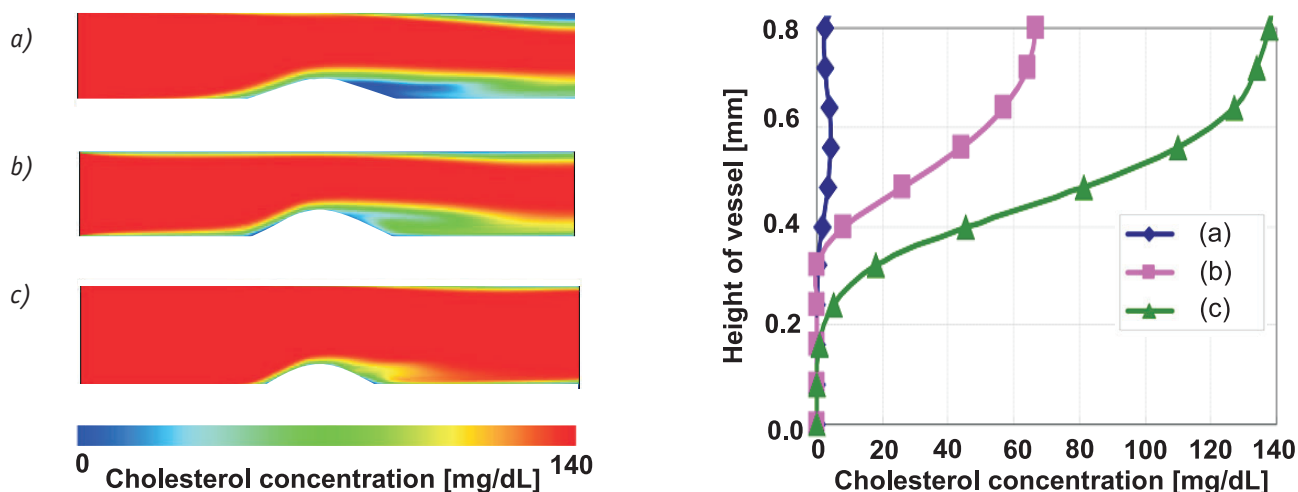


Fig. 6. Effect of vessel condition on cholesterol distribution in the blood tube (left) and in “beh ind coarctation area” shown in Fig. 2 at peak systole (right). (a) NBP and elastic vessel, (b) NBP and nonelastic vessel, and (c) HBP and elastic vessel.

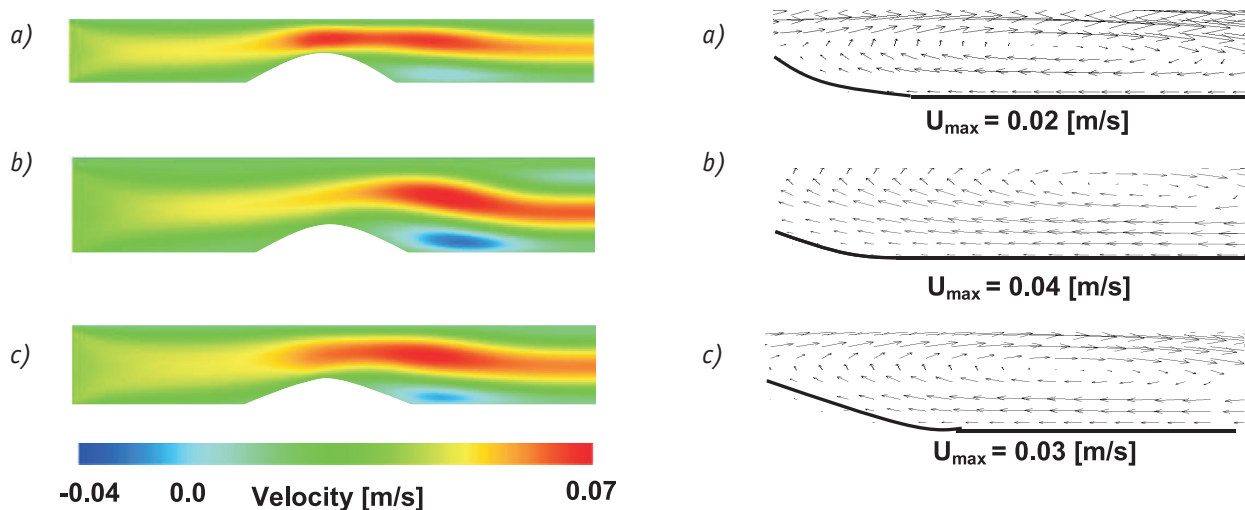


Fig. 7. Effect of vessel condition on velocity distribution (left) and its enlarged view in “behind coarctation area” shown in Fig. 2 at peak diastole (right). (a) NBP and elastic vessel, (b) NBP and nonelastic vessel and (c) HBP and elastic vessel.

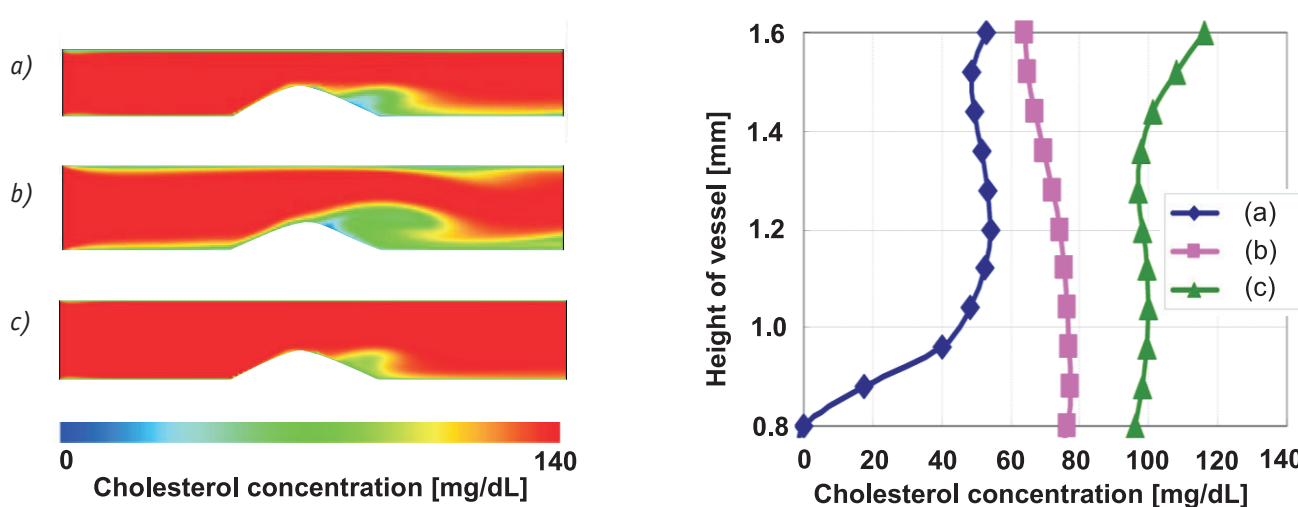


Fig. 8. Effect of vessel condition on cholesterol distribution in the blood tube (left) and in “behind coarctation area” shown in Fig. 2 at peak diastole (right). (a) NBP and elastic vessel, (b) NBP and nonelastic vessel, and (c) HBP and elastic vessel.

This result shows that cholesterol concentration changes between the peak systole (1.1 s) and the peak diastole (1.3 s) in the cases of (a) and (c). Because the blood flow suppresses the coarctation, cholesterol concentration becomes high value between peak systole. However, the coarctation expands at the peak diastole to decrease blood flow rate. Therefore, dead space appears behind the coarctation area and cholesterol concentration decreases in this area. Vessel diameter and back flow velocity of (b) remained constant values and they were larger than those of (a) (Figures 5 and 7). Therefore, cholesterol concentration of (c) is higher than that of (a).

#### 4. Conclusions.

A simulation code for calculating velocity distribution and cholesterol distribution in a blood tube with coarctation under various vessel conditions has been developed. The numerical results showed the followings:

- (1) Reverse flow appeared behind the coarctation.
- (2) Cholesterol was transported to behind of the coarctation area by the reverse flow.
- (3) HBP and noelastic vessel wall had a significant effect on the blood flow and cholesterol distribution.

#### AUTHORS

**Masashi Naito\*** - Department of Material Sciences & Chemical Engineering, Shizuoka University, 3-5-1 Johoku, Naka-ku, Hamamatsu, 432-8561, Japan.

E-mail: f0930200@ipc.shizuoka.ac.jp.

**Kensaku Mizoguchi** - Department of Material Sciences & Chemical Engineering, Shizuoka University, 3-5-1 Johoku, Naka-ku, Hamamatsu, 432-8561, Japan. Present address; Science Academy of Tsukuba, Tsukuba International Congress Center, 2-20-3 Takezono, Tsukuba, 305-0032, Japan.

**Youhei Takagi** - Department of Material Sciences & Chemical Engineering, Shizuoka University, 3-5-1 Johoku, Naka-ku, Hamamatsu, 432-8561, Japan.

**Yasunori Okano** - Energy System section, Graduate School of Science and Technology, Shizuoka University, 3-5-1 Johoku, Naka-ku, Hamamatsu, 432-8561, Japan.

\* Corresponding author

#### References

- [1] Torii R. *et. al.*, "Numerical investigation of the effect of hypertensive blood pressure on cerebral aneurysm - Dependence of the effect on the aneurysm shape", *Int. J. Numer. Meth. Fluids*, no. 54, 2007, pp. 995-1009.
- [2] Kim T., Ley O., "Numerical Analysis of the cooling Effect of Blood Over Inflamed Atherosclerotic Plaque", *Trans ASME J. Biomech. Engineering*, no. 130, 2008, 031013.
- [3] Sugawara M., *et. al.*, "Relationship between the pressure and diameter of the carotid artery in humans", *Heart Vessels*, 15, pp.49-51 (2000).
- [4] Oshima M., *et. al.*, "Modeling of inflow boundary conditions for image - based simulation of cerebrovascular

flow", *Int. J. Numer. Meth. Fluids*, no. 47, 2005, pp. 603-607.

#### Nomenclature

|                |  |                       |
|----------------|--|-----------------------|
| $a_0$          | : modification coefficients                      | [ - ]                 |
| $a_n$          | : Fourier cosine coefficient                     | [ - ]                 |
| $b_n$          | : Fourier sine coefficient                       | [ - ]                 |
| $c$            | : cholesterol concentration                      | [ mg/dL ]             |
| $c_0$          | : base cholesterol concentration (140)           | [ mg/dL ]             |
| $C$            | : dimensionless cholesterol concentration        | [ - ]                 |
| $D$            | : diffusion coefficient                          | [ m <sup>2</sup> /s ] |
| $E$            | : Young's modulus                                | [ Pa ]                |
| $h$            | : thickness of vessel wall                       | [ m ]                 |
| $L_{movement}$ | : movement of vessel wall                        | [ m ]                 |
| $n$            | : term number of fourier series                  | [ - ]                 |
| $p$            | : pressure                                       | [ Pa ]                |
| $P_i$          | : timedependent blood pressure                   | [ mmHg ]              |
| $P_{base}$     | : baseline blood pressure value                  | [ mmHg ]              |
| $P_{blood}$    | : blood pressure value                           | [ mmHg ]              |
| $r$            | : radius of vessel                               | [ m ]                 |
| $t$            | : time   | [ s ]                 |
| $u$            | : velocity in horizontal direction               | [ m/s ]               |
| $u_i$          | : inlet velocity of blood flow                   | [ m/s ]               |
| $U$            | : dimensionless velocity in horizontal direction | [ - ]                 |
| $v$            | : velocity in vertical direction                 | [ m/s ]               |
| $V$            | : dimensionless velocity in vertical direction   | [ - ]                 |
| $x$            | : coordinate in horizontal direction             | [ - ]                 |
| $X$            | : coordinate in horizontal direction             | [ - ]                 |
| $y$            | : coordinate in vertical direction               | [ - ]                 |
| $Y$            | : coordinate in vertical direction               | [ - ]                 |
| $\varepsilon$  | : strain   | [ - ]                 |
| $\Delta P$     | : difference of blood pressure                   | [ N/m <sup>2</sup> ]  |
| $\Delta t$     | : time step                                      | [ s ]                 |
| $\nu$          | : kinematic viscosity                            | [ m <sup>2</sup> /s ] |
| $\sigma$       | : stress   | [ N ]                 |
| $S_c$          | : Schmidt number                                 | [ - ]                 |